Published in final edited form as:
Chem Commun (Camb). 2013 November 28; 49(92): 10874–10876. doi:10.1039/c3cc45414b.

Enhanced Single Molecule Fluorescence and Reduced Observation Volumes on Nanoporous Gold (NPG) Films

Yi Fu, **Jian Zhang**, **Kazimierz Nowaczyk**, and **Joseph R. Lakowicz**
Center for Fluorescence Spectroscopy, University of Maryland School of Medicine, 725 W. Lombard Street, Baltimore, MD, USA.

Yi Fu: yfu@umaryland.edu

Abstract

We report single molecule fluorescence studies on nanoporous gold films. We observed dramatically enhanced intensities from individual immobilized fluorophores and reduced effective observation volumes in the nanopores. The overlaid mapping image derived from surface reflectance and fluorescence emission visualizes the enhanced localized plasmon field existing in the "nanovoid" regions.

It is now well known that plasmonic excitations in metallic nanostructures allow concentrating optical fields within deep-subwavelength volumes and are able to dramatically enhance molecular fluorescence intensities[1–3]. The result of an enhanced local electromagnetic field surrounding the metallic nanostructure is a strong function of physical parameters such as nanoparticle size, shape and coincidence between the nanoparticle resonance wavelength and the dye absorption/emission wavelength. Enhanced near-field electromagnetic fields near metallic nanostructures owing to localized surface plasmons can alter optical properties like emission intensity and lifetime of fluorophores in the vicinity of metallic interfaces. Numerous nanostructures have recently been developed as possible substrates for plasmon-controlled fluorescence (PCF)[1,3,4]. Such nanostructures are promising for trace molecular detections and diagnoses because of the significant improved quantum efficiency of the probes.

In this paper, we discuss the fluorescence enhancement induced by nanoporous gold (NPG) film. Free-standing NPG films with nanoporous channels are of particular interest owing to high surface-to-volume ratio, excellent chemical stability and biocompatibility[5–10]. Small gold colloids are typically quenchers of fluorescence. As the particle size increases gold can enhance fluorescence, especially of longer wavelength fluorophores[11–14]. NPG films are typically fabricated by dealloying of binary alloys, especially the Au-Ag alloy[6,15,16]. In the dealloying process, silver component is selective dissolved from the alloy frame, leads to an

Correspondence to: Yi Fu, yfu@umaryland.edu.

†Electronic Supplementary Information (ESI) available: Experimental details of NPG fabrication, immobilization procedures and single molecule experiments. Separate scanning images of reflectance and fluorescence from the same sampling region. TCSPC Analysis of single molecule lifetime, and analysis of Fluorescence correlation spectroscopy autocorrelation. See DOI: 10.1039/b000000x/

open bicontinuous network comprised almost entirely of gold. The gold surface can be made hydrophobic or hydrophilic by coating with appropriate thiol functional groups. Therefore it is likely that NPG will be practical as a PCF substrate[7,17–23].

In this study, NPG films with the thickness of ~100 nm were fabricated by dealloying the 12 carat gold leaves in concentrated HNO_3 (supporting information S1–2). The SEM image of an as-prepared NPG film in Figure 1 illustrates the “sponge”-like spatial nanostructure which consists of interconnected ligaments with curvatures. Most of ligaments exhibits elongated geometries in one direction and formed nanopores are distributed roughly 20–30 nm in width. Cy5 fluorophores were immobilized on NPG film by reacting of trace quantity of Cy5 succinimidyl ester with primary amine to the NPG surface which was modified by 2-aminoethanethiol (Supporting information S1). During the experiments, single molecule measurements and fluorescence correlation spectroscopy (FCS) were used to characterize the photophysical behaviors of probe molecules inside the porous structures.

The comparison of scanning confocal fluorescence images provides the initial facts of enhanced fluorescence. The apparent emission intensities from single Cy5 molecules on glass are generally less than 40 cps. These emission spots are hardly observable under the contrast scale as shown in Figure 1. On the contrary, the brightness of emission spots significantly increases on NPG films as shown in the image. Most of bright spots in the image correspond to the fluorescent signal from one Cy5 probe as evidenced by the increased spot density accompanied with higher incubation dye concentrations. To be certain that the investigated bright spots arise from single dye molecules and not from gold nanostructure scattering or other optical process, we have investigated time trajectories for these emission spots (Figure 2a). The “on-off” intermittency signals and the abrupt one-step photobleaching illustrated in Figure 2a are characteristic of single molecule behaviors. Using the same incident excitation power, we observed significantly higher emission rate from the molecules on the NPG substrates as compared to the control samples on glass substrate. The time profiles presented are representative of more than half of those emission spots in the scanned images and illustrate the overall trend observed from around 50 single molecules on two different substrates, respectively. The distribution of fluorescence emission rates measured on NPG surfaces is more variable than those measured on glass, showing asymmetric Gaussian distribution, indicating the heterogeneity of the nonporous structures. In fact, the single molecules randomly experienced the possible enhancements when take into account the distribution and enhancement of the electric field in the exceptionally disordered nanopores, occurring at assorted immobilization positions and orientations on the NPG surfaces. Nevertheless, much higher overall brightness was observed on NPG films, which are generally more than 15-fold from those observed on glass.

We also implemented the time-correlated single photon counting (TCSPC) measurement on a single fluorescent spot (supporting information S3–4).The nearly single exponential decay of fluorescence observed for different molecules in the absence of metal suggests that most of the molecules adsorbed on glass are in a relatively homogeneous environment. In the NPG porous structure, double exponential decay analysis yields two decay components. The multi-component decay suggests variations in the photonic mode density around the probe.

However, the intensity amplitudes differ considerably. We observed a predominant intensity contribution (90%) from the fast lifetime component for the investigated single molecules located in NPG. The results confirm that the interaction of the excited molecule with the nanostructure increases the radiative decay rate that results in shortened excited state lifetimes and enhances emission rates due to the energy transfer mechanism.

Additionally, we have performed simultaneous reflectance and fluorescence imaging of immobilized Cy5 probes on the NPG film with the diffraction limited spatial resolution. Scanning confocal fluorescence imaging of the sample slide was first performed to obtain fluorescence distribution map with relative higher immobilized probe concentrations (100nM). Then, the same sample area was mapped by reflected scattering light to reveal its rough surface features. Figure 3 illustrates an overlaid mapping image of fluorescence intensity and reflectance from the same scanning region (supporting information Figure S3). The increase in the molecule brightness by raising the extent of labeling is not favorable in this case due to self-quenching, as we did not observe the possible higher brightness comparing with the maximal value of the single molecule fluorescence. However, when correlated the intensity image to its surface morphology reflectance image, it appears that high intensity regions only arise from locations close to gaps or “nanovoid” spaces of the substrate. Despite the strong fluorescence observed proximity to nanovoids, we can rarely find intense emission arising from the relatively smooth regions on this highly porous sample. It has been proved that the surface plasmons in the voids of porous metal films are very strongly localized and the enormous resonant light absorption occurs at the plasmon resonance of the void network[19,21,24,25]. We assume that intensively localized void plasmons in a thin layer of porous metal would strongly interacting with surface plasmons, which can greatly enhance excitation light and alter radiative decay rates of nearby fluorophores. As the plasmon-enhanced fluorescence (PEF) is due to the interaction of excited fluorophores with surface plasmons from the noble metals, which leads to increased radiative rates, coupling to metal surface plasmons, and scattering into the far field, the fluorescence intensity mapping implies that highly localized surface plasmons occur at narrow interstices or on protrusions. The strong electromagnetic fields appear in the vicinity of gold ligaments due to the large curvatures of the ligament and nanopores. The strong near-field coupling could also arise from the narrow interstices between adjacent nanopore units. At smaller pores, the gap plasmon coupling becomes more dominant compared with the curvature effect, resulting in some “hot spot” regions[26]. For a very small fluorophore-metal distance, there is a quenching effect, the interaction of excited fluorophores with plasmons dominating at very close distances can be observed as fluorescence quenching. Self-quenching could also occur at relatively heavier labeling. However, self-quenching of the heavily immobilized probes can be partially eliminated by proximity of the fluorophores to the “hot spot” regions with the PCF effect [27].

We further examined the dynamic behaviors of fluorescent molecules near the nanopores. With the aids of the reflectance images, we were able to perform FCS with the focusing spots as close to the “void” regions as possible. The emission from the dye molecule can be quenched or enhanced when the molecule diffuse near the gold nanostructures, which could result in an obvious fluctuations occurring in the focal volume (Supporting information Figure S4). There are obvious stronger fluorescence bursts in the time traces, which are

probably due to the diffusion of dye molecules into the plasmonic near-field in the NPG pores where the molecule fluorescence is enhanced considerably. The effective detection volume and the number of molecules within the nanopores can be estimated from the correlation amplitude. There is an apparent increase in the amplitude value (G(0)) in NPG, the increase in the G(0) value implies more concentrated confocal optical fields near the nanopores and suggests that either few molecules are detected or additional sources of fluorescence fluctuation in the focal volume in NPG pores affects the FCS autocorrelation curves. The comparison of G(0) values reveal a roughly 20-fold reduction in the effective detection volume. Additionally, the decay of the autocorrelation curve of the NPG is also steeper than for the free diffusing solution (Figure 4 insert), indicating a reduction in the correlation time of the dye molecule, as depicted by a shift of the normalized autocorrelation function profile towards a shorter lag time. As the diffusion coefficient of the fluorophore is unchanged, the decrease in the diffusion time should be related with the reduction in the effective detection volume. The reduced effective detection volume and the improved brightness would certainly enhance the detectablity of the single diffusing molecules.

The development of plasmonic substrates to improve the detectability of single molecules and sensitivity has drawn massive interest for fluorescence sensing application. In this study, we have demonstrated the remarkable fluorescence enhancement of single fluorophores immobilized on NPG films. The strong enhanced localized surface plasmon–fluorophores coupling has been visualized by the mapping the intensity distribution over the surface morphology. Additionally, we observed decreased effective detection volumes in the nanopores, which are of great importance to increase detection sensitivity and consequently FCS at high concentrations. Nanopores have been successfully employed as a new tool to rapidly detect single biopolymers. Our studies have implied the novel opportunities to incorporate nanoporous metal substrates for both single-molecule and many molecule DNA assays in a flow-through platform.

Supplementary Material

Refer to Web version on PubMed Central for supplementary material.

Acknowledgments

This work was supported by NHGRI (HG002655, HG005090), NIBIB (EB006521, EB009509).

Notes and references

1. Lakowicz JR, Ray K, Chowdhury M, Szmacinski H, Fu Y, Zhang J, Nowaczyk K. Analyst. 2008; 133:1308. [PubMed: 18810279]
2. Lakowicz JR. Analytical Biochemistry. 2005; 337:171. [PubMed: 15691498]
3. Ming T, Chen HJ, Jiang RB, Li Q, Wang JF. Journal of Physical Chemistry Letters. 2012; 3:191.
4. Kinkhabwala A, Yu ZF, Fan SH, Avlasevich Y, Mullen K, Moerner WE. Nature Photonics. 2009; 3:654.
5. Seker E, Reed ML, Begley MR. Materials. 2009; 2:2188.
6. Zielasek V, Jurgens B, Schulz C, Biener J, Biener MM, Hamza AV, Baumer M. Angewandte Chemie-International Edition. 2006; 45:8241.

7. Ciesielski PN, Scott AM, Faulkner CJ, Berron BJ, Cliffel DE, Jennings GK. Acs Nano. 2008; 2:2465. [PubMed: 19206280]
8. Qian LH, Yan XQ, Fujita T, Inoue A, Chen MW. Applied Physics Letters. 2007:90.
9. Wittstock A, Biener J, Baumer M. Physical Chemistry Chemical Physics. 2010; 12:12919. [PubMed: 20820589]
10. Zhang L, Lang XY, Hirata A, Chen MW. Acs Nano. 2011; 5:4407. [PubMed: 21627303]
11. Fu Y, Zhang J, Lakowicz JR. Journal of the American Chemical Society. 2010; 132:5540. [PubMed: 20364827]
12. Mohammadi A, Sandoghdar V, Agio M. New Journal of Physcis. 2008; 10:105015.
13. Nakamura T, Hayashi S. Japanese Journal of Applied Physics Part 1-Regular Papers Brief Communications & Review Papers. 2005; 44:6833.
14. Xie F, Baker MS, Goldys EM. Chemistry of Materials. 2008; 20:1788.
15. Ding Y, Kim YJ, Erlebacher J. Advanced Materials. 2004; 16:1897.
16. Dixon MC, Daniel TA, Hieda M, Smilgies DM, Chan MHW, Allara DL. Langmuir. 2007; 23:2414. [PubMed: 17249701]
17. Lang XY, Guan PF, Fujita T, Chen MW. Physical Chemistry Chemical Physics. 2011; 13:3795. [PubMed: 21203619]
18. Hiep HM, Yoshikawa H, Taniyama S, Hoa LQ, Kondoh K, Saito M, Tamiya E. Japanese Journal of Applied Physics. 2010:49.
19. Sardana N, Heyroth F, Schilling J. Journal of the Optical Society of America B-Optical Physics. 2012; 29:1778.
20. Ruffato G, Romanato F, Garoli D, Cattarin S. Optics Express. 2011; 19:13164. [PubMed: 21747470]
21. Chen HA, Long JL, Lin YH, Weng CJ, Lin HN. Journal of Applied Physics. 2011:110.
22. Lang XY, Guan PF, Zhang L, Fujita T, Chen MW. Applied Physics Letters. 2010:96.
23. Qian LH, Das B, Li Y, Yang ZL. Journal of Materials Chemistry. 2010; 20:6891.
24. Bosman M, Anstis GR, Keast VJ, Clarke JD, Cortie MB. Acs Nano. 2012; 6:319. [PubMed: 22148628]
25. Teperik TV, Popov VV, de Abajo FJG, Kelf TA, Sugawara Y, Baumberg JJ, Abdelsalem M, Bartlett PN. Optics Express. 2006; 14:11964. [PubMed: 19529622]
26. Lang XY, Qian LH, Guan PF, Zi J, Chen MW. Applied Physics Letters. 2011:98.
27. Lakowicz JR, Geddes CD, Gryczynski I, Malicka J, et al. J. Fluoresc. 2004; 14:425–441. [PubMed: 15617385]

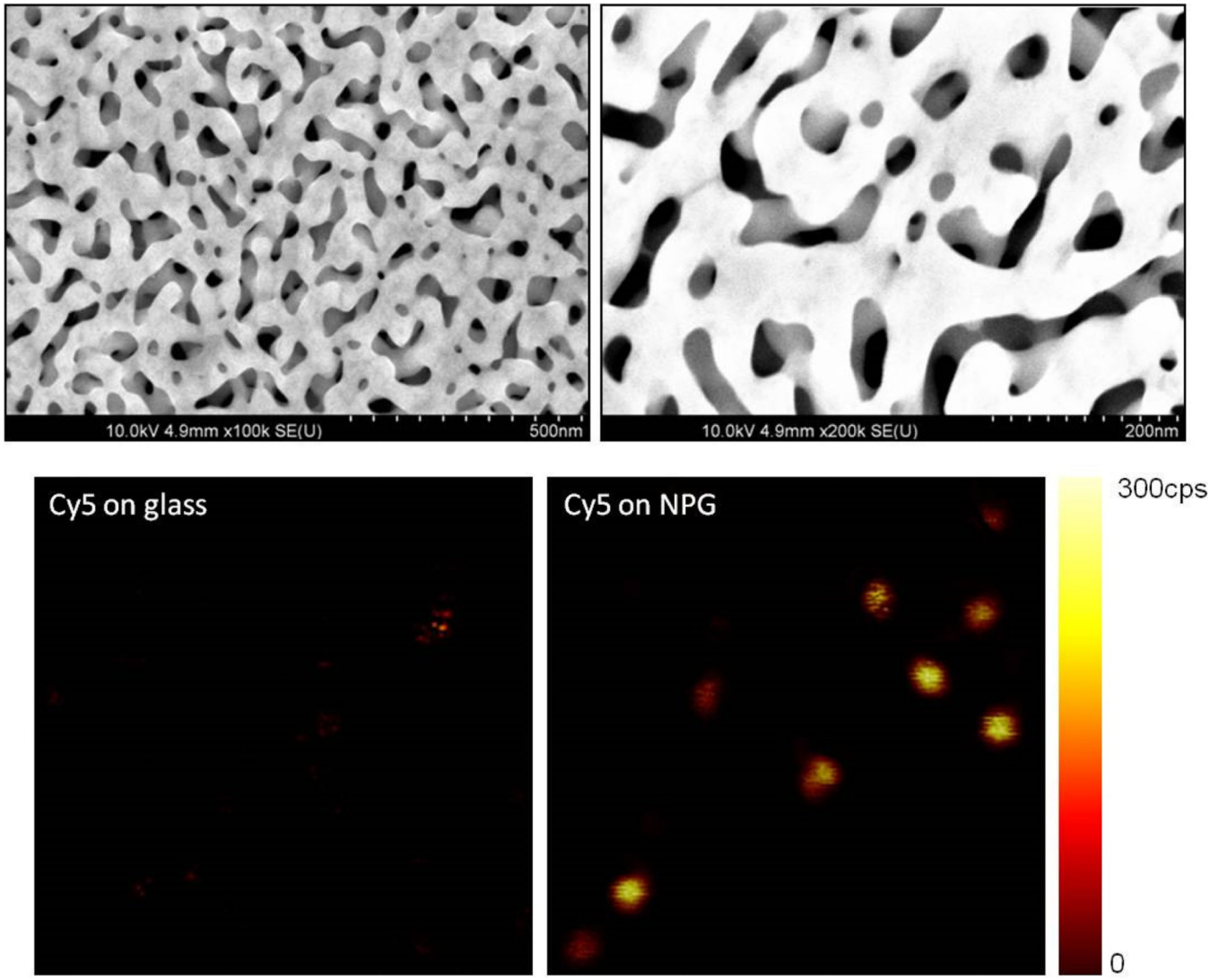

Figure 1.

(Top) SEM images of as-prepared NPG films with different scales. (Bottom) Confocal fluorescence images (10×10 μm of immobilized single Cy5 molecules on glass (left) and NPG (right), respectively.

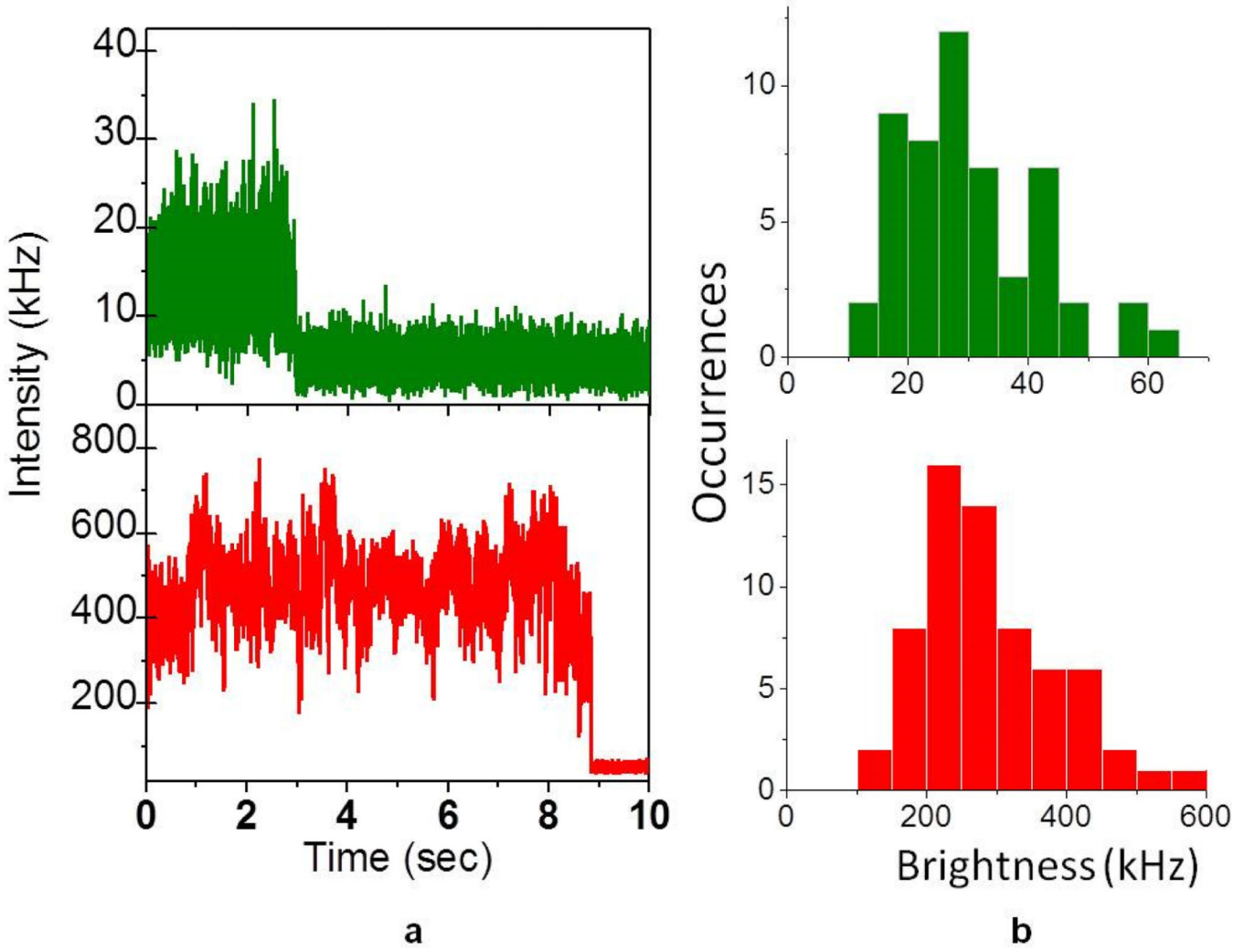

Figure 2.

(a) Single molecule trajectories of Cy5 immobilized on glass (green) and on NPG (red). (b) Histograms of emission rates collected from over 50 single fluorophores on glass (green) and on NPG (red).

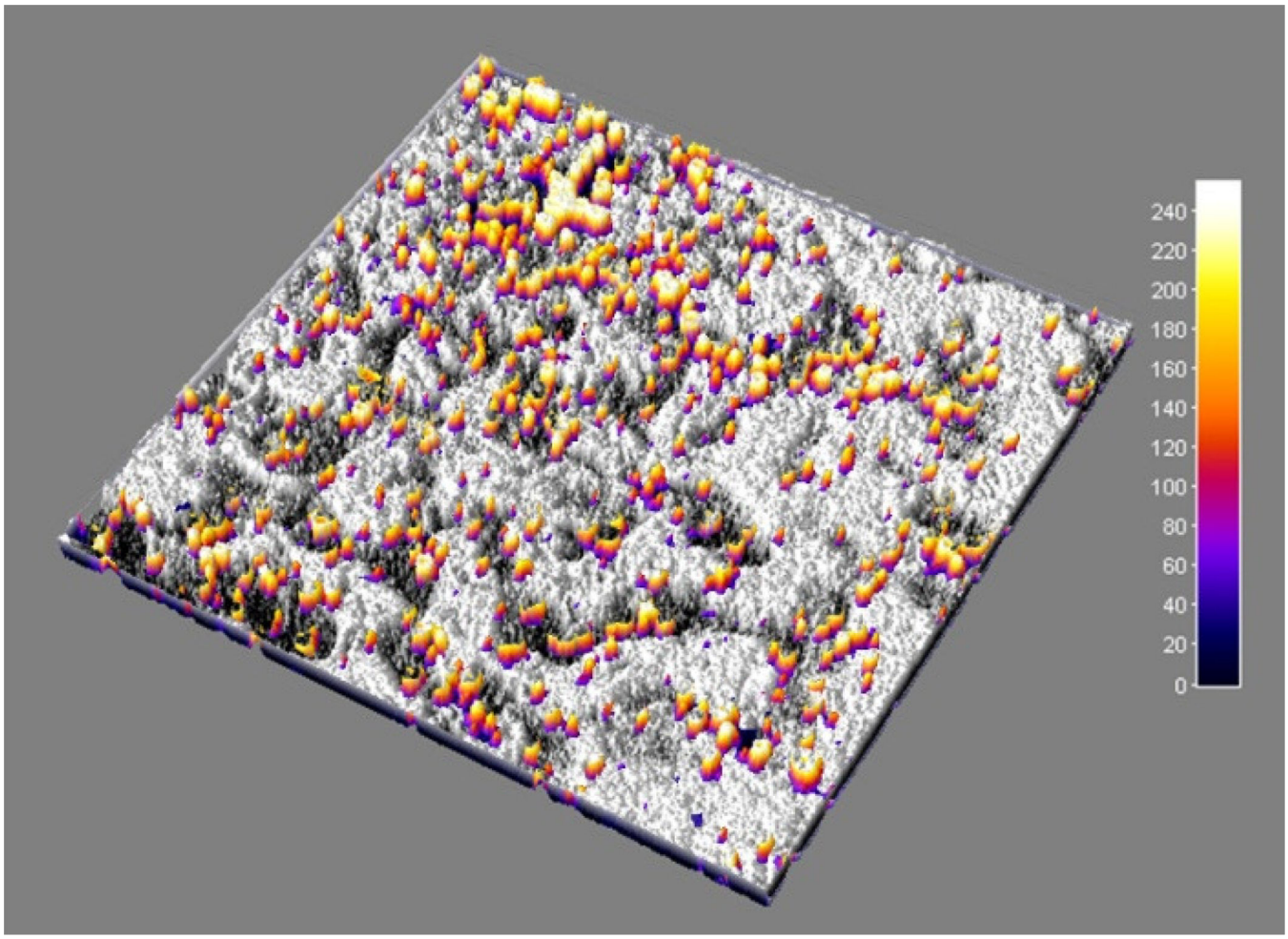

Figure 3.

An overlaid image (40×40 μm) of fluorescence emission over a surface contour on a NPG film. The shaded contour represents surface feature derived the reflectance image recorded from the same region.

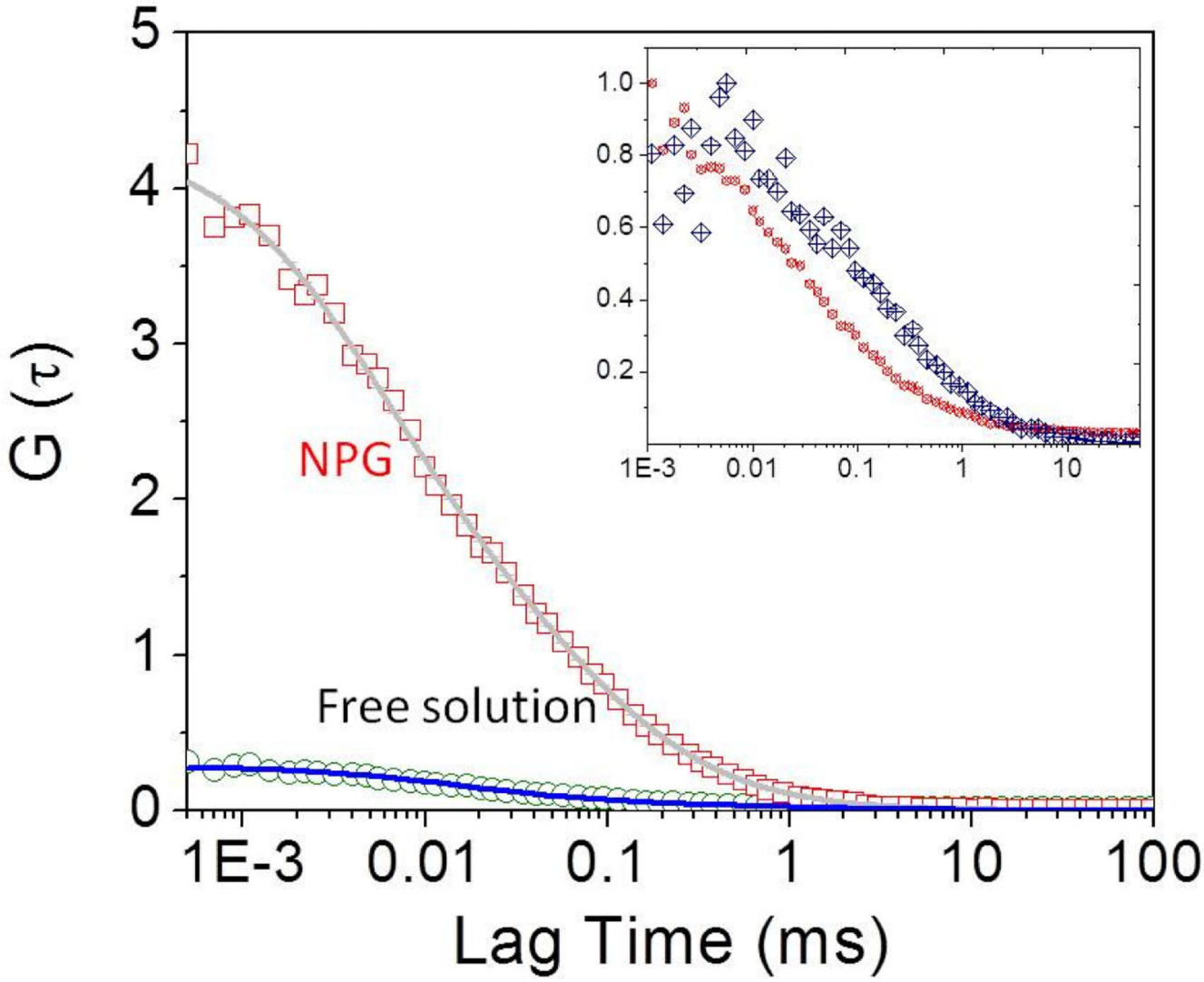

Figure 4.

Autoccorelation curves of 10 nM Cy5 molecules on a coverslip (open volume, free solution) and a NPG film. The insert shows the corresponding normalized autocorrelation (red: NPG; black: free solution).